doi:10.1093/plphys/kiab436 PLANT PHYSIOLOGY 2021: 187: 2716–2730

Plant Physiology®

Research Article

Vacuolar fructose transporter SWEET17 is critical for root development and drought tolerance

Marzieh Valifard,[1] Rozenn Le Hir,[2] Jonas Müller,[3] David Scheuring ,[3] Horst Ekkehard Neuhaus [1] and Benjamin Pommerrenig [1,*†]

1 Department of Plant Physiology, University of Kaiserslautern, Kaiserslautern, 67653, Germany
2 Institut Jean-Pierre Bourgin, INRAE, AgroParisTech, Université Paris-Saclay, Versailles, 78000, France
3 Department of Plant Pathology, University of Kaiserslautern, Kaiserslautern, 67653, Germany

*Author for communication: pommerre@bio.uni-kl.de
†Senior author.
M.V., H.E.N., and B.P. designed the research. M.V., R.L.H., J.M., and D.S. performed research. H.E.N. and B.P. wrote the article.
The author responsible for distribution of materials integral to the findings presented in this article in accordance with the policy described in the Instructions for Authors (https://academic.oup.com/plphys/pages/general-instructions) is: Benjamin Pommerrenig (pommerre@bio.uni-kl.de).

Abstract

Root growth and architecture are markedly influenced by both developmental and environmental cues. Sugars integrate different stimuli and are essential building blocks and signaling molecules for modulating the root system. Members from the SUGAR WILL EVENTUALLY BE EXPORTED TRANSPORTER (SWEET) family facilitate the transport of different sugars over cellular membranes and steer both inter and intracellular distribution of sugars. SWEET17 represents a fructose-specific sugar porter localized to the vacuolar membrane, the tonoplast. Here, we analyzed how SWEET17-dependent fructose released from vacuoles affects root growth during drought stress in Arabidopsis (*Arabidopsis thaliana*). We found that the *SWEET17* gene was predominantly expressed in the root vasculature and in meristematic cells of the root tip. SWEET17 expression appeared markedly induced during lateral root (LR) outgrowth and under drought. Moreover, fructose repressed primary root growth but induced density and length of first order LRs. Consistently, *sweet17* knock-out mutants exhibited reduced LR growth and a diminished expression of LR-development-related transcription factors during drought stress, resulting in impaired drought tolerance of *sweet17* mutants. We discuss how SWEET17 activity integrates drought-induced cellular responses into fructose signaling necessary for modulation of the root system and maximal drought tolerance.

Introduction

Sugars fulfill a wide number of different functions in plants. For example, they provide cellular energy required for many metabolic reactions and they serve as carbon precursors for numerous anabolic processes. In addition, sugars are necessary for modifications of proteins and membrane lipids, they accumulate as compatible solutes upon onset of osmotic-, salt-, or freezing stress and they contribute as quenchers to tolerate reactive oxygen species (Lineberger and Steponkus, 1980; Crowe et al., 1988; Sheen et al., 1999; Hoekstra et al., 2001; Ruan, 2014; Keller et al., 2021). Given that sugars fulfill so many different functions it is not surprising that the concentrations of various types of sugars are sensed and plants adjust nuclear gene expression accordingly (Rolland et al., 2002, 2006). Such sugar-modified alterations of gene expression cause subsequent changes in the development and metabolism (Rolland et al., 2002; Hanson and Smeekens, 2009; Steinbeck et al., 2020). Factors influencing sugar concentrations are, for example, modifications of the sugar provision by photosynthesis or

Received May 27, 2021. Accepted August 17, 2021. Advance access publication September 16, 2021

mobilization of storage compounds, sugar consumption for starch and cellulose synthesis, and modifications of energy metabolism or of the rates of anabolic reactions.

In cells, sugars are hydrated giving them solubility and prevent their free permeation across biological membranes. Accordingly, various individual sugar transport proteins mediate either, facilitated diffusion along an existing concentration gradient, or an energy-dependent transport driven by a proton-motive force across the individual membrane (Chen et al., 2015a, 2015b). A remarkable characteristic of the plant genome is the presence of a large number of individual genes coding for three major sugar transporter groups, namely MST-type monosaccharide transporters (MSTs), SUT-type sucrose transporters, and the Sugars Will Eventually be Exported Transporters (SWEETs)-type proteins (Sauer, 2007; Chen et al., 2015a, 2015b; Pommerrenig et al., 2018). Members from these transporter families steer both inter and intracellular distribution of sugars and their substrate specificities and diverse spatiotemporal expression patterns enable plants to allocate sugars to the right place at the right time to initiate developmental or stress-related responses (Eom et al., 2015; Julius et al., 2017; Pommerrenig et al., 2020).

Interestingly, in recent years alterations of the intracellular sugar compartmentation and their effect on developmental processes gained more attention (Wingenter et al., 2010; Klemens et al., 2013; Guo et al., 2014; Klemens et al., 2014; Pommerrenig et al., 2018; Patzke et al., 2019; Rodrigues et al., 2020). Such changes in the intracellular sugar compartmentation can in particular be induced by alterations of the activity of vacuolar membrane (tonoplast) located transport proteins (Hedrich et al., 2015). This is, because the vacuole is the largest cell organelle and a major function of this organelle is the regulation of dynamic sugar storage processes (Martinoia et al., 2007, 2012). Apart from a direct effect of sugar levels on the expression of genes involved in photosynthesis (Koch, 1996) altered sugar levels strongly govern plant organ properties (Hanson and Smeekens, 2009). These sugar coordinated processes range from effects on (1) early plant germination and development of the vasculature, (2) onset of flowering, (3) modifications of fruit yield, and (4) size or morphology of plant organs (Tjaden et al., 1998; Takahashi et al., 2003; Dekkers et al., 2004; Weichert et al., 2010; Wahl et al., 2013; Le Hir et al., 2015).

The Arabidopsis genome harbors in total 17 isoforms of proteins belonging to the SWEET family (Chen et al., 2012; Eom et al., 2015). Our current understanding is, that from 17 SWEET isoforms in Arabidopsis only three locate to the vacuolar membrane, namely SWEET2, 16, and 17 (Chardon et al., 2013; Klemens et al., 2013; Chen et al., 2015a, 2015b). While most SWEET proteins analyzed exhibit a quite low substrate specificity and mediate transport of glucose, fructose, and sucrose, SWEET17 turned out to be specific for fructose transport as confirmed by both, direct transport assays and analyses on corresponding Arabidopsis loss-of-function mutants (Chardon et al., 2013; Guo et al., 2014). Gene expression studies indicated that *SWEET17* mRNA is relatively abundant in root cells, although the impact of the corresponding transporter activity on root-associated processes still remains unclear (Guo et al., 2014).

Given that sugars are known to modulate root development (Takahashi et al., 2003), given that intracellular sugar compartmentation influences many cell and organ characteristics (see above) and given that *SWEET17* mRNA is highly abundant in root cells it was of particular interest to search for an impact of SWEET17 transporter activity on root properties. To this end, we studied the effect of sugars on root architecture and analyzed the cell-specific *SWEET17* gene expression in more detail. We found that the *SWEET17* gene is specifically strong expressed at positions of the primary root (PR) where lateral roots (LRs) emerge. In the course of our work, we identified fructose as an inducer of genes required for LR formation and that *sweet17* mutant plants exhibit impaired LR formation. These characteristics are most likely responsible for an observed limited drought tolerance of *sweet17* plants, which goes along with induction of the *SWEET17* gene under conditions of low soil–water availability. In summary, we propose that SWEET17 is a cellular component required for proper root development and involved in maximal drought tolerance of Arabidopsis.

Results

Fructose inhibits primary and induces LR growth

It is widely known that sugars not only affect processes like flower induction, fruit yield, and fruit quality but also the development of plant organs (Tjaden et al., 1998; Wingenter et al., 2010; Ruan, 2012; Wang and Ruan, 2013; Lastdrager et al., 2014). Thus, we were interested to search for specific effects of different types of sugars on root development. To this end, we grew Arabidopsis wild-type (WT) plants (Col-0) for 14 d on half-strength MS (1/2 MS)-agar medium supplemented with either 0.8% of mannitol (to check for osmotic effects), sucrose, glucose, fructose, or without any sugar supplements (MS-0) and recorded parameters defining the root system architecture (RSA; Figure 1). Plants grown on MS-0 produced ∼5 cm long PRs with only few and very short first-order LRs during the time tested. The addition of mannitol to the agar medium did not induce visible changes of the RSA in comparison to MS-0 grown plants, whereas supplementation with glucose, fructose, or sucrose changed RSA substantially (Figure 1A). Interestingly, these three sugars acted differently on PR and LR growth (Figure 1, B–D). While glucose and sucrose stimulated growth of PRs, fructose rather inhibited this process (Figure 1B). Indeed, PRs of plants grown with sucrose were on average twice as long and those of plants grown with glucose were 50% longer than PRs of plants grown on MS-0 or mannitol (Figure 1B). Interestingly, fructose, in contrast to glucose or sucrose, inhibited PR growth by ∼30% in average, when compared to PR length from controls (Figure 1, A and B).

When compared to the MS-0 and mannitol treatments sucrose, glucose, and fructose all markedly induced the

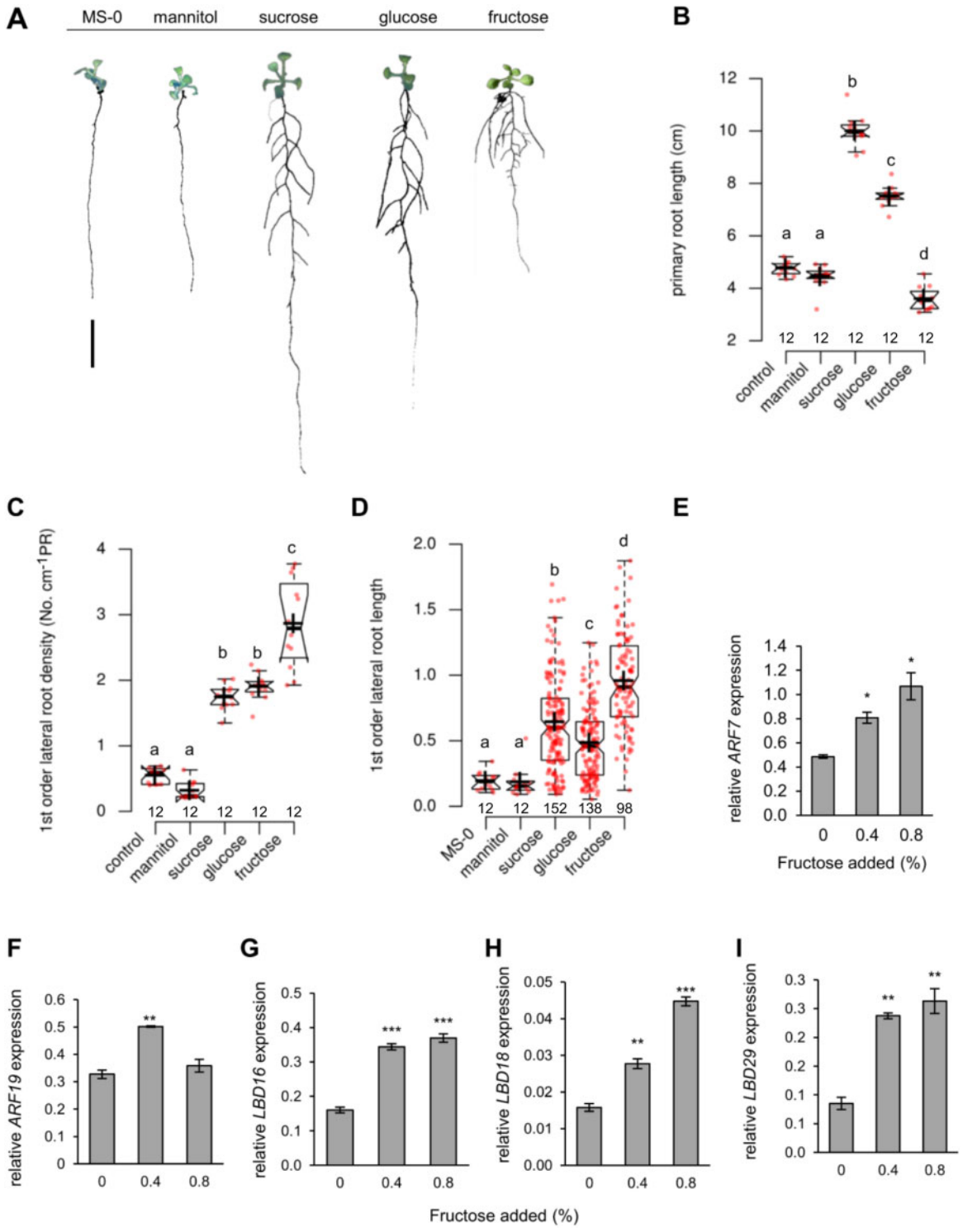

Figure 1 Plasticity of root growth of WT plants in response to different sugars. A, Representative pictures of plants grown on MS agar plates without (control) or supplemented with 0.8% of corresponding sugars or mannitol and grown for 10 d. Bar = 1 cm (B) PR length (C) First order LR density of plants grown with different sugars (D) First order LR length. Different letters above boxes denote significant differences according to *one-way* ANOVA with post-hoc Tukey HSD test ($P < 0.05$). Center lines within boxes show the medians; crosses show means; box limits indicate the 25th and 75th percentiles; whiskers extend 1.5 times the interquartile range (IQR) from the 25th and 75th percentiles, outliers are represented by dots. Notches are defined as $\pm 1.58 \times$ IQR/sqr(n) and represent the 95% confidence interval for each median. Numbers below boxes indicate sample size. E–I, Fructose-dependent expression of transcription factor genes involved in LR formation in WT plants. Seeds were germinated and plants grown on MS agar plates supplemented with the indicated fructose concentrations. Roots from 2-week-old seedlings were used for gene expression analysis. Bars are means from $n = 3$ replicates. Each replicate represents pooled roots from eight plants. Error bars are SE (one-way ANOVA/Duncan $P < 0.05$) and asterisks indicate significant differences in comparison to control (0% fructose added). Expression levels of *ARF7* (E), *ARF19* (F), *LBD16* (G), *LBD18* (H), and *LBD29* (I) are shown.

emergence of LRs resulting in significantly increased first order LR density along the PR (Figure 1C). The average LR length under control conditions was ~0.2 cm, while the presence of glucose or sucrose led to an LR length of ~0.5 cm and 0.7 cm, respectively (Figure 1D). The most marked fructose effect was obvious when we quantified the average LR length of plants grown in the presence of this sugar. Fructose stimulated LR growth strongly, leading to an average length of 0.9 cm (Figure 1C).

Moreover, we analyzed fructose effects on the expression of several genes required for LR initiation and elongation, namely *AUXIN RESPONSE FACTOR7 and 19* (*ARF7* and *ARF19*), and *LATERAL ORGAN BOUNDARIES-DOMAIN16, 18 and 29* (*LBD16*, *LBD18*, *and LBD29*) which all represent genes coding for proteins required for LR emergence and growth (Okushima et al., 2005, 2007; Péret et al., 2009; Bellini et al., 2014). Interestingly, the levels of the corresponding mRNAs were increased in roots in a fructose-dependent manner (Figure 1, E and G–I). In contrast to the above genes, which all showed maximal expression at 0.8% fructose, *ARF19* mRNA was highest at a fructose concentration of 0.4%.

To characterize fructose-specific changes in root architecture (impaired PR length and stimulated LR length) further, we grew Arabidopsis seedlings on 1/2 MS containing 0.8% sucrose (control) and increased the additionally given fructose between 0.02% and 0.32%. The already present sucrose promoted LR formation (Supplemental Figure S1A) leading to a presence of ~13 LR per plant. Under these conditions, the additional fructose application led to an increase of the number of LRs reaching a maximum of ~15 LR per plant already at 0.02% fructose, and a decreased number of LRs at 0.32% fructose (11 LR per plantSupplemental Figure S1B). Similar to the observations above, the presence of fructose stimulated LR length. From 0.04% fructose on, a significant increase of LR length was measurably reaching a maximum at ~0.32% (Supplemental Figure S1C). Although higher fructose concentrations provoked a decrease of the PR length (Supplemental Figure S1D), it appears remarkable that at 0.02% fructose, representing a concentration which induced the highest number of newly emerged LRs (Supplemental Figure S1B), the length of the PR was also similar when compared to control conditions (Supplemental Figure S1D).

Fructose-dependent inhibition of PR growth is less pronounced in *sweet17* mutants when compared to WT

As demonstrated above, fructose-induced specific effects on the root architecture, when compared to other types of majorly abundant sugars (Figure 1, A–C). Thus, we were interested to reveal whether alterations in cellular fructose compartmentation cause changes in root morphology.

From all Arabidopsis MSTs analyzed so far, only one homolog is fully specific for fructose transport, namely, the tonoplast located transporter SWEET17 (Chardon et al., 2013; Guo et al., 2014). Therefore, given that fructose stimulates the emergence and length of LRs we were interested to see whether the effect of fructose on root growth would differ between WT plants and *sweet17* loss of function mutants (Chardon et al., 2013). When grown on MS agar plates without any sugar supplementation (Ms-0) WT and the two tested *sweet17* mutants (*sweet17-1 and sweet17-2*, see Chardon et al., 2013) did not differ in their PR lengths. When grown on 2% fructose, WT plant responded with a reduction of PR growth to ~50% of the length grown under MS-0 (Figure 2). This inhibition was stronger when compared to the situation observed with 0.8% fructose supplementation (Figure 1). Interestingly, the fructose-dependent inhibition of PR growth of *sweet17-1 and sweet17-2* mutant plants was less severe when compared to WT plants. PR growth of *sweet17-1* mutants was decreased to ~60% and that of *sweet17-2* mutants to ~65% of the growth on MS-0 (Figure 2). These data indicated that the fructose-derived repression of PR growth was—at least in part—influenced by the SWEET17 protein.

The *SWEET17* gene is expressed at positions of emerging LRs

In previous work, we demonstrated that the expression of the *SWEET17* gene in source leaves is generally low and mainly confined to the vasculature (Chardon et al., 2013). To analyze cell-specific activity of the *SWEET17* promoter, we expressed a *ProSWEET17-RPL18*-green-fluorescent protein (*GFP*) gene construct, which encodes a fusion of the open reading frame of the GFP with the ribosomal protein RPL18, preventing intercellular trafficking of the GFP from its site of biosynthesis (Figure 3, A–F). Recording of the GFP-derived fluorescence indicated *SWEET17* promotor activity in the cortex and the vasculature of primary and LRs (Figure 3). Only a faint GFP fluorescence could be detected in cortex cells (Figure 3C). Within the vasculature we detected fluorescence mainly in cells adjacent to the pericycle cell layer (Figure 3A). These fluorescing cells comprised different phloem and xylem cells most likely including differentiating proto and metaxylem cells (Figure 3A). GFP fluorescence was obvious and strong in cells in close vicinity to LR primordia (LRP; Figure 3, B and C). At later stages of LR emergence, GFP-fluorescence was mainly detected throughout the vasculature (Figure 3E) and in an even later stage only in the LR tip in cells including and surrounding the quiescent center (Figure 3F).

This localization pattern agreed with GUS staining of roots from *ProSWEET17-GUS* plants (Chardon et al., 2013) grown on 1/2 MS-agar media (Figure 3G). The analyses revealed that *SWEET17* expression in roots mainly occurs in the vasculature and that this expression is particularly strong at locations where LRs emerge from the PR (Figure 3G). Already before LR formation was obvious, the GUS activity driven by the *SWEET17* promotor allowed identification of the positions where these secondary root structures emerge (Figure 3G). GUS staining was visible after ~6–10 h of incubation of the freshly harvested plants in GUS staining solution in the early phase of LR formation while at later stages

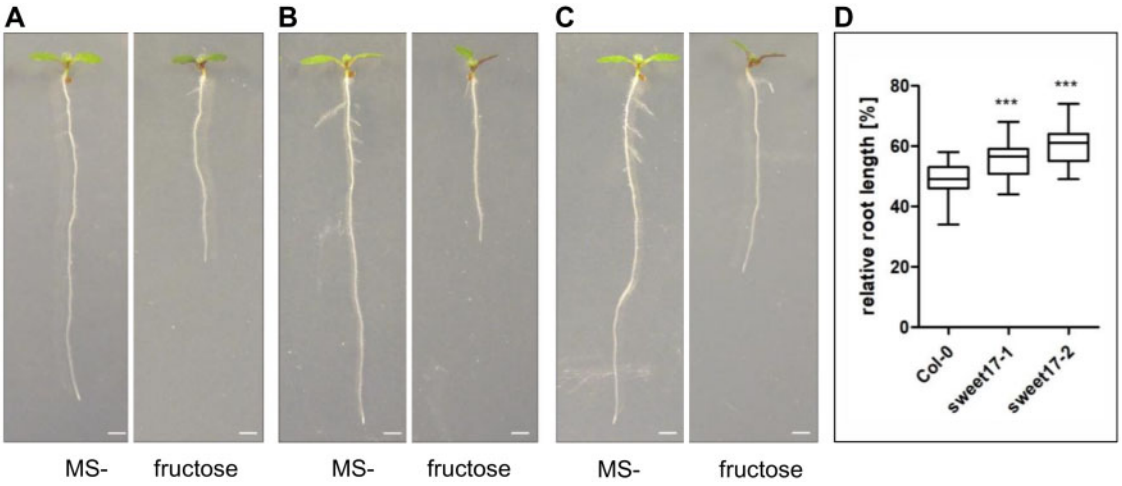

Figure 2 Relative root growth on fructose. Seven-day-old *Arabidopsis* seedlings were grown on 1/2MS without sugar (MS-) and with 2% fructose, respectively. The inhibitory effect of fructose on the mutants *sweet17-1* (B) and *sweet17-2* (C) was analyzed and compared with the Col-0 WT (A). D, Boxplots showing relative root length of fructose-grown Arabidopsis seedlings (Col-0 $n = 32$, *sweet17-1* $n = 18$, and *sweet17-2* $n = 19$) based on root growth on MS-. Quantification of root length after 7 d. Center lines within boxes show the medians; box limits indicate the 25th and 75th percentiles; whiskers extend 1.5 times the IQR from the 25th and 75th percentiles. Asterisks indicate significant differences from Col-0 according to one-way ANOVA followed by Dunnet's post-hoc test. *P*-values: ***$P < 0.001$. Bars are 1 mm.

staining was mainly present at the LR tip (Figure 3G; Supplemental Figure S2). GUS-staining in cross sections of the differentiation zone of LRs confirmed the observed GFP fluorescence in the vasculature (Supplemental Figure S2).

It is worth to mention that the *SWEET17* gene expression in the root vasculature observed here (Figure 3) extents earlier observations using a 2,700 bp long *SWEET17*-promotor fragment fused to GUS in which GUS staining was detected already after 2 h of staining in cortex cells (Guo et al., 2014). Such pattern could be confirmed for the closely related SWEET16 (Guo et al., 2014), which exhibited GUS staining mainly found in the root cortex and not in the vasculature (Supplemental Figure S2). The cell type-specific expression pattern *SWEET17* recorded by the GFP and GUS reporters overlapped with cell-specific microarray data where expression of SWEET17 was strongest the vasculature of roots and comparably weaker in the cortex cells (Brady et al., 2007; Winter et al., 2007; Cartwright et al., 2009; Supplemental Figure S3).

The *SWEET17* gene is drought-induced

One of the main functions of roots is the supply of the plant with water and the root system exhibits an impressive ability to alter its architecture in response to drought (Comas et al., 2013; Koevoets et al., 2016). To check for a putative function of SWEET17 activity in this process we grew Arabidopsis in a hydroponic system and applied drought stress by the addition of polyethylene glycol (PEG) 8000, to reach an osmotic potential of −0.5 MPa. After the first 6 h of drought, *SWEET17* expression dropped to ∼25% of the control value at the beginning of the experiment (Figure 4A). However, within the next 6 h a rapid increase of the corresponding mRNA was obvious, reaching 3 times the value present at 0 h drought stress (Figure 4). This high *SWEET17* mRNA level lasted for another 12 h and maintained high, leading to ∼200% of the 0 h value after 36 h of drought (Figure 4A). The drought-induction of *SWEET17* was also visible by GUS staining of LRs of corresponding *ProSWEET17-GUS* plants grown under control or −0.5 MPa conditions (Supplemental Figure S2). To check for a possible functional redundancy of SWEET16 and SWEET17 during drought we analyzed the *ProSWEET16-GUS* (Guo et al., 2014) and *ProSWEET17-GUS* plants at control and drought conditions. These analyses revealed that *SWEET16 and SWEET17* expression patterns did not overlap (Supplemental Figure S2). While GUS staining of our *ProSWEET17-GUS* line was strongest in the vasculature of the roots, the *ProSWEET16-GUS* lines showed GUS staining mainly in the cortex. The contrasting expression patterns were even more pronounced in plants exposed to drought stress. While roots of drought-exposed *ProSWEET17-GUS* plants displayed stronger staining in comparison to *ProSWEET17-GUS* plants grown at control conditions, such effect was not observed for *ProSWEET16* plants (Supplemental Figure S2). While *SWEET17* expression was clearly induced by the applied drought conditions in the hydroponic medium (Figure 4A), this was not the case for *SWEET16*. In fact, *SWEET16* expression was rather downregulated during drought 3 h after application of the stress and stayed low for another 24 h, a time when *SWEET17* expression levels were already greatly induced (Figure 4; Supplemental Figure S4).

SWEET17 loss-of-function mutants exhibit decreased tolerance against drought stress and increased drought-dependent fructose accumulation

To check for an effect of missing SWEET17 activity on plant performance under drought we grew WT and *sweet17-1* mutants for 3 weeks in the hydroponic culture medium and

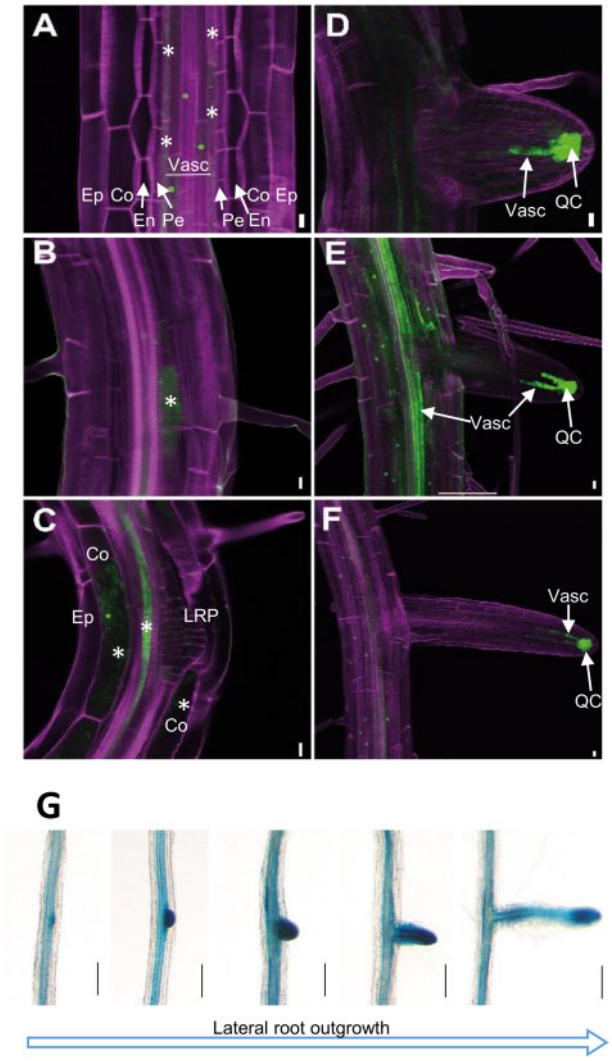

Figure 3 *ProSWEET17: HF-RPL18-GFP* seedlings were grown for 7 d in 1/2 MS medium. A–F, Confocal images of different stages of LR development. In (A–C), pictures are single confocal optical sections plane and in (D–F), pictures are maximum intensity images from stacks of confocal optical sections. The calcofluor and GFP fluorescence are color-coded in magenta and green respectively. Co, cortex; Ep, epidermis; En, endodermis; QC, quiescent center and surrounding cells; Pe, pericycle; Vasc, vascular system. Scale bars represent 10 µm. Asterisks marks GFP fluorescence in cells adjacent to the pericycle layer (A), in cells in close vicinity to LRP (B and C), and in the cortex (C, Co). G, Histochemical localization of *ProSWEET17-GUS* activity during LR formation at different developmental stages detected from a root of single plant. *ProSWEET17-GUS* seedlings were grown for 14 d in MS medium followed by staining for GUS activity. Bars are 40 µm.

induced drought by the addition of PEG8000 (−0.5 MPa). We applied the stress stimulus for up to 5 d and quantified shoot and root dry mass from a representative number of plants in 24 h intervals. At the beginning of the experiment, WT plants exhibited an average shoot dry weight of 16 mg/plant (Figure 4B). Right after onset of drought, WTs arrested shoot growth, as the dry weight did not increase until the second day after exposure to drought (Figure 4B). From there, WT plants restarted growth gaining ∼10% of shoot biomass daily (Figure 4B). *sweet17-1* plants exhibited only 70% of the WT shoot dry weight at the beginning of the experiment, namely ∼11 mg/plant (Figure 4B). Similar to WTs net dry weight accumulation stopped during the first 2 d after onset of drought and restarted within the next 3 d. However, the relative shoot biomass gain was only ∼6% per day and therefore less than in WT (Figure 4B).

After cessation of root growth for 1 d after transfer to drought conditions, WT root biomass increased markedly at a rate of ∼45% or 1.6 mg per plant and day. In contrast to WT, roots from *sweet17-1* mutant gained only ∼25% of their root mass at the start of the experiment or 0.5 mg per plant and day during drought (Figure 4C). The differential shoot and root biomasses accumulation kinetics of WT and *sweet17-1* mutant plants during drought resulted also in altered root to shoot ratios of the two plant lines. While root to shoot ratio of WT increased 2.5-fold during the 5 d of drought, this ratio increased only 1.8-fold in *sweet17-1* plants (Figure 4D).

It is known that leaves from *sweet17* loss-off-function plants contain high levels of fructose (Chardon et al., 2013). However, so far it is unknown whether the same holds true for roots. A corresponding analysis is, moreover, of interest since fructose exhibited effects on root architecture (Figure 1) and modified expression of genes required for drought-induced root differentiation (Figure 1, E–I).

In general, the onset of drought caused a marked increase of the contents of glucose, fructose, and sucrose in roots of both WT and *sweet17-1* mutants (Figure 4E). At the beginning of the experiment, the levels of glucose and fructose in roots from WT and *sweet17-1* plants were comparable, and amounted to ∼5 µmoles glucose/g FW and ∼2 µmoles fructose/g FW (Figure 4E). The sucrose contents of roots were at the beginning of the experiment extremely low in both genotypes and did not exceed 0.1 µmoles/g FW (Figure 4E). Interestingly, the glucose levels in *sweet17-1* mutant roots and WT roots changed with marked similarity, while fructose levels in *sweet17-1* roots were, after onset of drought, nearly always substantially higher when compared to WT levels (Figure 4D). Quantification of sucrose showed that *sweet17-1* roots exhibited (with the exception at Day 2) always less of this type of sugar when compared to WT (Figure 4E).

sweet17 loss-of-function mutants exhibit impaired root development under control and drought conditions

Given that fructose induce specific effects on the root architecture (Figure 1, A–D) and that *sweet17* mutants exhibit blockage of fructose export from the vacuole (Chardon et al., 2013), we were interested to analyze whether alterations in cellular fructose compartmentation cause changes in root morphology. Thus, to study root architecture for longer times we grew all Arabidopsis lines in hydroponic culture medium. After 18 d of growth, both *sweet17* mutants exhibited decreased PR length of ∼90% of the length of WT PRs (Figures 5, A and C). LRs from *sweet17-1* and *sweet17-2* plants reached 1.7 cm on average, representing about two-

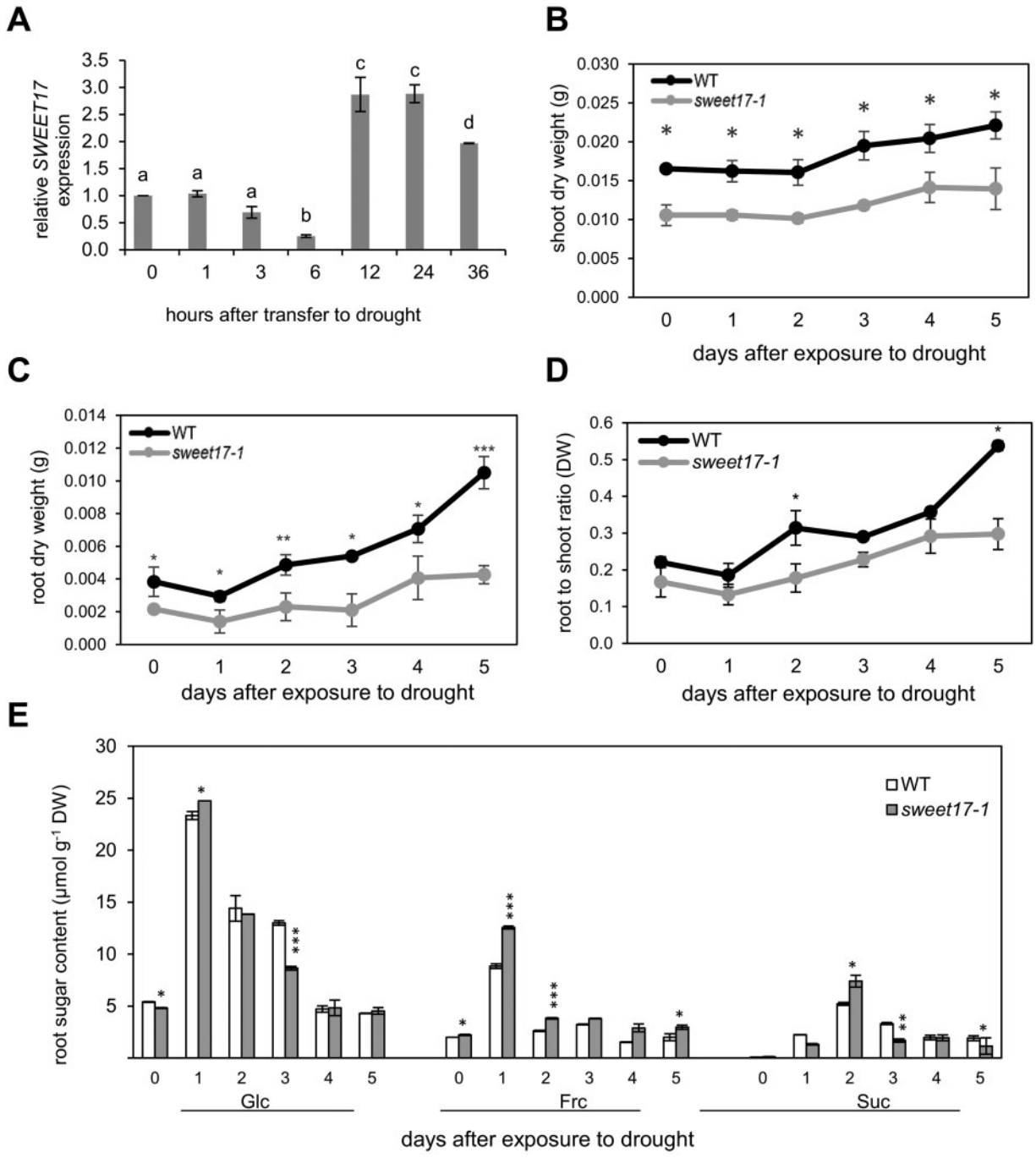

Figure 4 Drought-induced expression of *SWEET17* and response of *sweet17-1* mutant plants to short-term drought stress. Plants were grown on hydroponic medium for 3 weeks and then seedlings exposed to drought stress produced by PEG8000 ($\Psi s = -0.5$ MPa). Samples were harvested at different time points after applying drought and used for RNA extraction, biomass, and sugar measurement. A, relative expression of *SWEET17*. Bars represent means from $n = 3$ biological replicates ± SE. Different letters above bars denote significant differences according to one-way ANOVA with post-hoc Duncan testing ($P < 0.05$). B–D, Development of shoot (B), root (C), and root:shoot (D) biomass of WT and *sweet17-1* mutant plants in response to short-term drought stress. Data points are means from n = five biological replicates ± SE (one-way ANOVA/Duncan $P < 0.05$). E, Root sugar content of WT and *sweet17-1* mutant plants grown under drought stress produced by PEG8000 ($\Psi s = -0.5$ MPa). Results are shown as representative of five independent plants. Bars are means from n = five biological replicates ± SE (one-way ANOVA/Duncan $P < 0.05$) and asterisks indicate significant differences from the WT.

third of the LR length of WTs (Figures 5, A and D). Similar to the difference in the average LR lengths, both *sweet17* mutant lines showed a lower number of LRs when compared to WT plants (Figure 5, A and E). Latter plants produced in average 23 LRs per plant, while *sweet17-1 and sweet17-2* plants generated only ∼20 and 18 LRs per PR, respectively (Figure 5E). When grown under drought, induced by the addition of PEG8000 leading to an osmotic potential

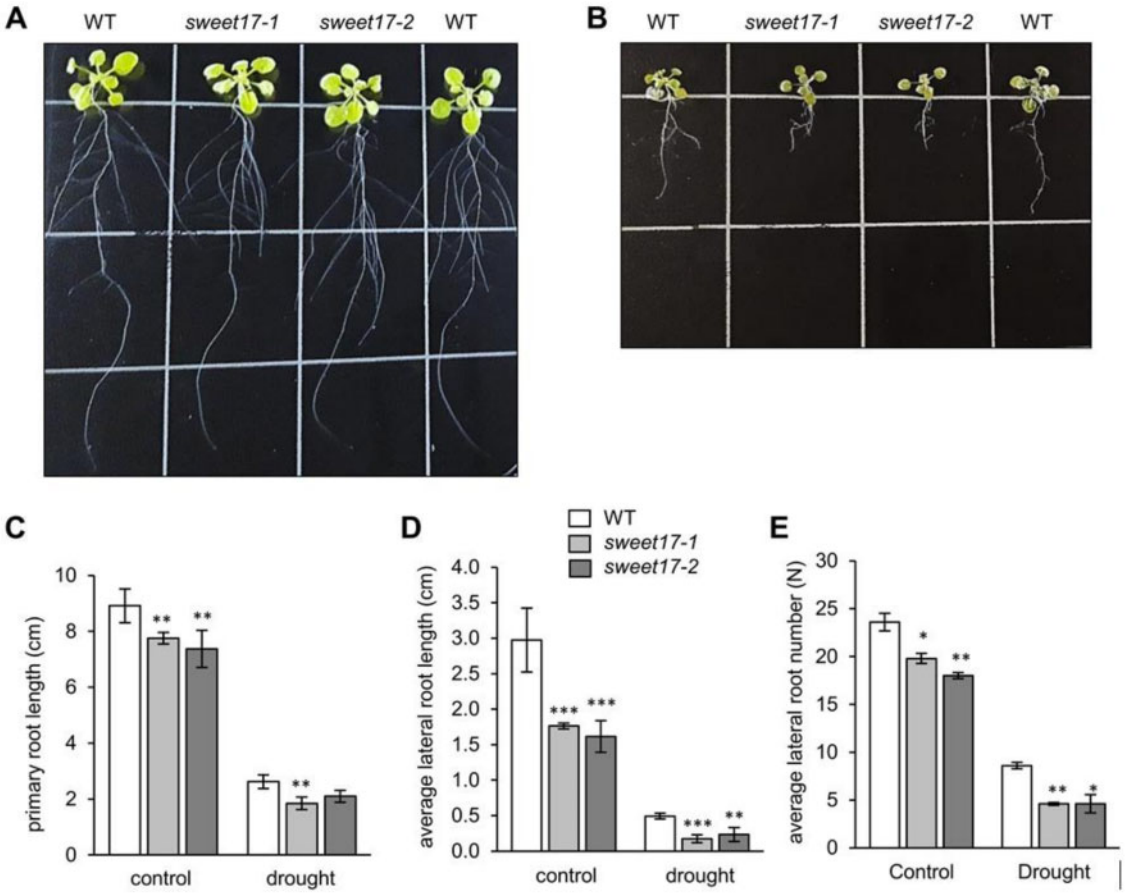

Figure 5 Root phenotypes of WT and *sweet17* mutant lines exposed to drought stress. A and B, Three-week-old plants grown in hydroponic media. One week after germination, growth media were exchanged with the experimental solution without (A) and with PEG8000 to produce −0.5 MPa osmotic potential mimicking drought (B). C–E, Quantification of root parameters. PR length (C), average LR length (D), and average lateral root number (E) were calculated. Bars show means of 10 independent plants ± SE. Asterisks indicate significant differences from the WT according to one-way ANOVA and Duncan test ($P < 0.05$).

of -0.5 MPa, the development of WT and *sweet17* mutant roots was impaired. WT plants produced in average ∼8.5 LRs per plant, while *sweet17-1 and sweet17-2* mutants both produced ∼4.5 LRs per plant (Figure 5, B and E). In comparison, drought reduced the emergence of LRs in WTs about three-fold, while LR formation in *sweet17-1* and *sweet17-2* mutant lines was reduced four- and three-fold, respectively (Figure 5E).

Given, that both *sweet17* mutants show impaired LR formation and reduced LR length, it was interesting to check for altered expression of genes critical for LR emergence and growth (Péret et al., 2009; Bellini et al., 2014). To this end, we quantified via reverse transcription quantitative (RT-qPCR) mRNAs encoded by the genes *LBD16*, *LBD29*, *ARF7*, *and ARF19*. It turned out, that in both *sweet17* loss-of-function lines the levels of the *LBD16*, *LBD29*, *ARF7*, and *ARF19* mRNAs were significantly lower when compared to corresponding levels in roots from WTs plants under control conditions (Supplemental Figure S5).

On soil, *sweet17* mutants show impaired drought tolerance properties

To check for an effect of loss of SWEET17 on long-term drought effects on soil substrate, WT and *sweet17* mutants were grown together for 1 week under well-watered control conditions and then drought, indicated by 60% or 40% water field capacities (FCs).

Under well-watered conditions (100% FC), WT and both *sweet17* mutant lines grew with the same efficiency (Figure 6A) reaching a shoot biomass of ∼1.5 g per plant after 5 weeks (Figure 6B). Interestingly, both *sweet17* mutant lines exhibited significantly greater problems to cope with the onset of drought, when compared to WT (Figure 6). After 5 weeks of growth at 60% FC shoot biomass of both, *sweet17-1- and sweet17-2* mutant plants was 25%–30% lower in comparison to WT plants (Figure 6C). At 40% FC, WT plants decreased their shoot biomass even further and reached only about one-tenth of the fresh weight gained at 100% FC. The drought-dependent reduction of shoot

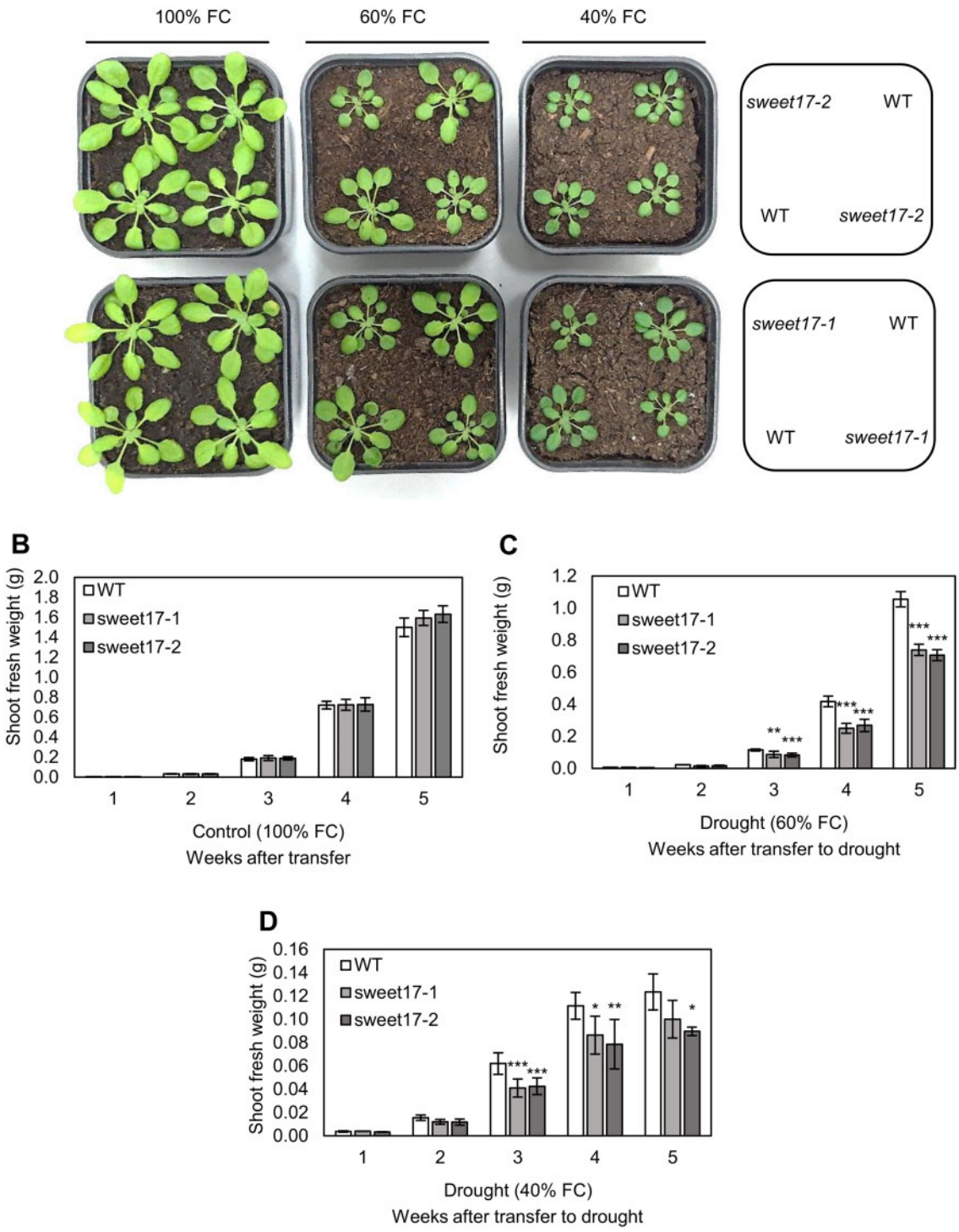

Figure 6 Arabidopsis WT and *sweet17* mutant growth in response to 3 weeks of drought stress. plant phenotype (A), shoot fresh weight of plants under well watered (B), moderate (C), and severe (D) drought conditions. Seeds were germinated on soil and 7-d-old seedlings were transferred to moderate drought conditions produced by 60% of soil FC, considered in two independent groups. In order to prevent high osmotic shock to young seedlings, the 40% FC (severe drought) was applied on the second group of plants that have been already grown under 60% FC for 1 week. Samples were harvested per week after applying drought. Results are means of five independent replicates. Error bars represent SE. Asterisks denote significant differences from WT according to one-way ANOVA with post-hoc Duncan test, $P < 0.05$).

biomass was again more drastic in both *sweet17-1- and sweet17-2* mutant plants reaching a net biomass of ~70% of that of the WT value after three and of ~80%–70% after 4 weeks of growth, respectively (Figure 6D). We always observed that the drought-dependent differences between WT and *sweet17* mutants became weaker with prolonged duration of the drought stress. Together these results showed that drought reduced growth of *sweet17* mutants to

a stronger degree than WT plants and indicated that impairments of SWEET17-dependent root formation corresponded with reduced drought tolerance of *sweet17* mutants.

Discussion

In many reports, it was shown that controlled intracellular sugar compartmentation is critical for plant development and yield, as well as for tolerance against biotic or abiotic stresses (Linke et al., 2002; Klotke et al., 2004; Bogdanovic et al., 2008; Jung et al., 2015; Chen et al., 2015a, 2015b; Pommerrenig et al., 2018; Keller et al., 2021). It seems, that one major reason for this multi-faceted impact of intracellular sugar compartmentation is the marked signaling function of different types of sugars (Rosa et al., 2009; Cho and Yoo, 2011; Granot et al., 2013) which governs gene expression—and by this—nearly all plant properties. Moreover, in contrast to other signaling molecules typically present at low abundance, sugars deliver in addition energy and metabolic precursors for numerous biosynthetic pathways. Only the presence of latter both factors allow stimulation of metabolism and simultaneous formation of novel cellular structures, required to induce developmental changes, and to build up stress tolerance (Keller et al., 2021).

It is known that sugar availability stimulates root development (Takahashi et al., 2003). In line with this observation we demonstrated that all three sugars analyzed, namely fructose, glucose, and sucrose stimulate the formation of LR with fructose being the most efficient stimulator of LR length growth (Figure 1, A and D). Latter result, received our further attention because Arabidopsis mutants lacking the tonoplast located sugar transporter SWEET17 exhibited a specific trapping of fructose in the vacuole of leaf mesophyll cells (Chardon et al., 2013; Guo et al., 2014), which led us speculate that SWEET17 activity might affect LR formation. This speculation gained further support by our observation that the *SWEET17* gene is markedly expressed in the central root vasculature (Figure 3) and that mutants lacking a functional SWEET17 protein exhibit altered root growth (Figures 2 and 5).

The finding that the *SWEET17* gene is expressed in the root vasculature (Figure 3) extends a previous report demonstrating *SWEET17* gene expression in root cortex cells (Guo et al., 2014). One reason for our contrasting observation might be the use of different promotor constructs. For both, the *ProSWEET17-GUS* (Chardon et al., 2013) and the *ProSWEET17-HF-RPL18-GFP* construct we used a *SWEET17* promotor element of ∼2,000 bp in length, while the *ProSWEET17-GUS* construct used in the previous study contained a promotor length of ∼2,700 bp (Guo et al., 2014). Latter promotor sequence might overlap with and contain regulatory elements of the promoter of the adjacent *At4g15930* gene, coding for a dynein light-chain type protein, which locates 3,000 bp distantly on the complementary strand. It is possible that regulatory elements within this region might drive the expression of SWEET17 in the cortex, which was absent from the Promotor-GUS lines used in our study. In addition, promotor activity is not only dependent on the exact promotor structure but largely on environmental factors like for example, light intensity and day length. In this context, it has to be mentioned, that one major difference between the expression experiments done by (Guo et al., 2014) and presented here is that we studied gene expression patterns on plants grown under short day, while Guo et al. (2014) analyzed gene expression on plants grown under long-day growth conditions. These two factors, different promotor lengths, and light regimes might contribute to the observed differences in the tissue-specific expression of *SWEET17*.

The vacuolar membrane, named tonoplast, harbors several different sugar transporters mediating import and export of various types of sugars (Hedrich et al., 2015). In contrast to all other tonoplast located sugar transporters analyzed, solely SWEET17 transports only one type of sugar, namely fructose (Chardon et al., 2013; Guo et al., 2014). The metabolic origin of vacuolar fructose is not fully resolved although a recent study indicates that a high vacuolar invertase activity leads to a release of fructose by sucrose hydrolysis (Vu et al., 2020). In any case, the observation that roots from *sweet17* mutants accumulate fructose, but not glucose or sucrose (especially when exposed to drought stress, Figure 4E) fully concurs with similar observations made on *sweet17* leaves (Chardon et al., 2013) and indicates that SWEET17 provides this type of sugar to the cytosol of corresponding cells.

The stimulatory effect of fructose on LR formation (Figure 1) goes well along with a fructose concentration-dependent increase of *ARF7 and ARF19*, as well as *LBD16*, *LBD18*, and *LBD29* mRNAs (Figure 1, C–I). ARF7 and ARF19 have been identified as two auxin response factors acting downstream of the initial hormone signaling and both proteins are required for cell cycle activation and proper cell patterning during LR initiation (Péret et al., 2009; Bellini et al., 2014). LBD16 and LBD18, as members of the LBD transcription factor family, are also critical for LR formation and their corresponding genes exhibit a marked expression during early initiation of LR (Lee et al., 2015, 2019), while the presence of LBD29 is required to allow LRP to breach through the root endodermis (Porco et al., 2016). Thus, the presence of fructose induces exactly the genes required for initiation of LR formation.

LR formation starts at a few pairs of so-called pericycle founder cells—located near the xylem pole—conducting cell division in anticlinal and asymmetric manner (Lavenus et al., 2013). It is known that local changes of the auxin tissue concentrations are required to pericycle founder cells to initiate this specific division pattern leading to an LRP (Jones and Ljung, 2012). Interestingly, various sugars like sucrose, glucose, and fructose induce auxin accumulation via two mechanisms, namely the induction of the expression of corresponding biosynthesis enzymes and stimulated expression of auxin transporter genes (Mishra et al., 2009; LeClere et al., 2010). Thus, for following reasons it seems feasible that the activity of

SWEET17 is involved in LR formation: (1) the expression of the *SWEET17* gene is particularly high in the differentiating proto and metaxylem cells that are in closest proximity to the pericycle founder cells (Figure 3). (2) mutants lacking a functional SWEET17 protein show decreased numbers of emerging LRs and impaired LR length (Figure 5). (3) roots from *sweet17* mutants exhibit decreased levels of *LBD16*, *LBD29*, *ARF7*, and *ARF19* mRNAs, known to encode proteins with critical relevance for LR formation (Péret et al., 2009; Bellini et al., 2014; Porco et al., 2016). (4) *sweet17* roots contain higher fructose levels when compared to WTs (Figure 4), pointing to a vacuolar trapping of this sugar which acts as an inducer of *LBD16*, *LBD29*, *ARF7*, *and ARF19* gene expression (Figure 1, E–I).

During adaptation to drought conditions the root architecture of vascular plants becomes strongly modified to maintain extraction of water from the soil (Comas et al., 2013). The observation that the expression of the *SWEET17* gene is induced by drought already after 12 h after onset of stress (Figure 4A) indicates an involvement of SWEET17 in corresponding changes of the root architecture. In fact, since *sweet17* plants show an aberrant root architecture when compared to WT under both, control and drought conditions (Figures 2 and 5) it was not surprising to see that these mutants exhibit significantly impaired ability to tolerate decreased FCs in the soil or decreased water potentials in hydroponics (Figures 4–6).

Generally, after onset of drought Arabidopsis roots start to decrease the number and size of the LR (Deak and Malamy, 2005; Xiong et al., 2006; Koevoets et al., 2016). This dynamic response allows plants to direct the flux of carbon from LR growth to PR growth leading to exploration of deeper horizons in soil. In fact, there are studies on different species indicating both, that a reduced number of LRs leads to increased drought tolerance and that the drought induced signal—causing decreased LR numbers and reduced LR length—is at least partially caused by increased abscisic acid (ABA; De Smet et al., 2003; Xiong et al., 2006; Zhan et al., 2015). The relative drought-induced decrease of LR formation was stronger in *sweet17* mutants when compared to WT plants (2.7-fold decrease in WT against 4.6-fold decrease in *sweet17*; Figure 5).

Therefore, we conclude that SWEET17 activity in the xylem parenchyma is required to create a signal keeping LR formation and LR growth active. By this, Arabidopsis can balance the drought ABA-induced signal to tune down LR formation and LR growth, with a reciprocal positive molecular stimulus. Obviously, to gain maximal drought tolerance two antagonistic signals have to be merged. One signal provokes a decrease of the LR number and length, while the other signal—partly influenced by SWEET17 activitystabilizes LR formation and increased LR length to a certain optimal extend.

Interestingly, our observation that plants with impaired LR formation and LR growth are in fact less tolerant to drought is fully in line with observation on Arabidopsis mutants exhibiting enhanced drought tolerance. Latter plants exhibit a markedly increased root system with more LRs (Yu et al., 2008), supporting our notion that counteracting the down-tuning of LR formation and LR development is important to achieve a maximal drought tolerance. In summary, SWEET17 activity in the xylem parenchyma seems to be part of this fine-tuning machinery required to withstand this challenging abitotic stress stimulus.

Materials and methods

Plant and growth conditions

WT and transgenic Arabidopsis (*Arabidopsis thaliana*) plants were grown under different growth conditions based on the experimental design and purpose. For soil experiments, seeds were sown in pots containing standard soil (ED-73; Einheitserde Patzer; Sinntal-Altengronau, Germany), stratified at 4°C for 48 h and then grown under short-day conditions (10-h light, 14-h dark) at 125 µmol quanta m^{-2} s^{-1} light intensity and 21°C. For hydroponic culture, seeds were germinated on detached and punctated lids from Eppendorf cups filled with germination medium agar (Conn et al., 2013). By this, roots of developing plants were allowed to grow through the lids into germination medium. After 1 week, the germination media as replaced gradually with basal nutrient solution (BNS; Conn et al., 2013). The hydroponic medium (BNS) was replaced periodically each week in order to keep nutrient concentration and pH relatively constant. For growth on agar plates, 1/2 MS medium was used for experiments with PEG and sugar treatments. For this purpose, seeds were surface-sterilized in 70% ethanol followed by sodium hypochloride and stratified in the dark for 48 h at 4°C for stratification. The MS medium contained 1/2 MS salts, 0.05% (w/v) MES, 0.5% (w/v) sucrose, and 0.8% (w/v) agar (adjusted to pH 5.7 with KOH). To analyze primary and LR length, ImageJ version 1.46 software was used. For RNA and sugar extractions, plant tissues were harvested and frozen immediately in liquid nitrogen. All samples were kept at −80°C until analysis.

Analysis of carbohydrates

Sugar quantification was performed by coupled enzymic test (spectrophotometric analysis) as described previously (Quick et al., 1989).

Drought stress

To investigate the effects of drought stress on plant performance, water stress was applied to soil, hydroponic, and agar plate cultures based on different methods. To apply drought stress in hydroponic condition, 4 week-old plants were exposed to −0.5 MPa osmotic potential produced by PEG 8000 (Michel, 1983). PEG-infused plates were used to create low water potential treatment (Verslues et al., 2005).

For soil experiments, plants were exposed to drought conditions based on soil FC (Bouzid et al., 2019). Plants were kept at the determined water content on soil (control, 70%,

50%, and 40% FC) by a 48 h interval of irrigation until harvesting. Seeds of WTs and mutant lines were germinated on standard soil (ED-73; Einheitserde Patzer; Sinntal-Altengronau, Germany) and plants were grown for 1 week prior to transfer to soil with 60% moisture/FC as compared to the well-watered soil (100%). To prevent osmotic shock, seedlings were not directly transferred from 100% to 40% FC. Instead, 2 week-old seedlings which were grown for 1 week at 100% and 1 week at 60% FC, were not watered until 40% moisture in the soil was reached. Afterwards, the level of soil moisture was kept constant by monitoring pot weight (with a precision balance and an accuracy of 0.01 g) in 48 h intervals (Xt). To calculate the FC of the soil, three pots were filled with the corresponding soil, followed by drying in an oven for 4 d at 60°C to determine the weight of dry soil (X0) in each pot. Consequently, three further pots were filled with the same amount of soil as described for drying followed by watering the soil until water saturation (Xf). Subsequent to this, pots were transferred to the growth chamber. After 48 h, pots were weighted again (Xt). The percentage for FC of the soil was calculated using the following formula; $[(Xt-X0)/(Xf-X0)] \times 100$ (Bouzid et al., 2019).

RT-qPCR

Total mRNA was isolated from roots of plants grown either hydroponically or in 1/2 MS agar plates. The NucleoSpin RNA Plant Kit (Macherey-Nagel, Düren, Germany) was used to extract total RNA and iScript cDNA Synthesis Kit (Bio-Rad, Hercules, CA, USA) was used for synthesis of cDNA. RT-qPCR was performed according to Wormit et al. (2006). The sequence of primers used for quantification of transcripts levels of *SWEET17*, *ARF19*, *ARF7*, *LBD16*, *LBD18*, and *LBD29* are documented as Supplemental Table S1. For transcript normalization, *PP2A* (*AT1G13320*) and *SAND1* (*AT2G28390*) were used as reference genes (Czechowski et al., 2005).

Histological localization of SWEET17

The tissue localization of ProSWEET17-GUS was analyzed by histochemical analysis of transgenic plants expressing *SWEET17* combined with GUS reporter gene. Transgenic plant tissues were stained with X-Gluc-containing solution according to Chardon et al. (2013). Tissue localization of ProSWEET17-GUS was observed by Nikon SMZ1111 stereomicroscope combined with a ProgResC3 camera and ProgResCapturePro version 2.8 software (JENOPTIK, Jena, Germany).

Generation of the pSWEET17-HF-RPL18-GFP Arabidopsis transgenic line

To generate an entry clone for the *SWEET17* promoter (2,004 bp) a recombination with Gateway® BP Clonase II Enzyme Mix (Thermo Fisher Scientific, Waltham, MA, USA; 11789-100, https://www.thermofisher.com) was performed between pDONR207 vector (Invitrogen Waltham, MA, USA) and the pKGWFS7 vector carrying the *SWEET17* promoter (Chardon et al., 2013). *ProSWEET17* was then introduced upstream of the HF-RPL18-GFP coding sequence (TMV omega 5′ leader (66bp) fused to an open reading frame that consists a FLAG epitope fused to the 187 amino acid coding sequence of RPL18B) by recombination with Gateway® LR Clonase II Enzyme Mix (Thermo Fisher Scientific, 11791-100, https://www.thermofisher.com) between pDONR207:proSWEET17 and the pGATA:HF-RPL18-GFP binary vector (Mustroph et al., 2009). Promoter sequence in the binary vector was verified by sequencing and the binary vector ProSWEET17:HF-RPL18-GFP was introduced into *Agrobacterium tumefaciens* strain C58pMP90 (Koncz and Schell, 1986) by electroporation. Arabidopsis was then transformed by the floral dip method (Clough and Bent, 1998). Six independent monoinsertional lines were selected on kanamycin (50 mg/L). They all displayed GFP fluorescence in the root. The T3 line expressing the strongest GFP signal was further analyzed.

Confocal imaging

Seedlings were fixed in PFA 4% for 30 min under vacuum and then for 1 h at 4°C. Incubation in PBS 1× twice 5 min allows to remove the fixative solution. Roots were then incubated overnight in a solution containing 0.1% calcofluor (w/v) in Clearsee solution prepared according to Ursache et al. (2018).

Roots were then mounted in Clearsee solution for observation under an SP8 confocal microscope (Leica, https://www.leica-microsystems.com/). Calcofluor and GFP were detected using laser lines at 405 and 488 nm, respectively. Intensities of the 405 and 488 nm lasers were set to 2% and 60%, respectively. The gain for both laser lines was <700. Calcofluor fluorescence emission was detected at 425–460 nm, and GFP fluorescence emission was detected at 495–520 nm. Depending on the pictures, a water-corrected 20× or 63× objective was used (HC PL APO CS2 20×/0.75 Oil/Gly/WATER, HC PL APO CS2 63×/1.20 WATER). Developing LRs were imaged as stacks of confocal optical sections and maximum intensity images were produced by ImageJ software (https://imagej.nih.gov/ij/) for each channel. Both channels were then merged to obtain the pictures presented in Figure 3.

Accession numbers

Accession numbers of analyzed genes are listed in Supplemental Table S1.

Supplemental data

The following materials are available in the online version of this article.

Supplemental Figure S1. Root growth profiles of WT in response to fructose treatments.

Supplemental Figure S2. GUS-Staining patterns of *PromotorSWEET16*-GUS and *PromotorSWEET17*-GUS plants in roots.

Supplemental Figure S3. Expression of *SWEET17* in roots according to single-cell microarray data.

Supplemental Figure S4. Expression of *SWEET16* in plants exposed to drought stress.

Supplemental Figure S5. Expression profiles of transcription factors responsive to LR formation in WT and *sweet17* lines exposed to drought stress.

Supplemental Table S1. Primers used for RT-QPCR.

Acknowledgments

The authors would like to thank Ruth Wartenberg and Ralf Pennther-Hager (University of Kaiserslautern) for their excellent technical assistance and plant growth. We also thank Dr. Françoise Vilaine (IJPB, Versaille, France) for important help in cloning the pSWT17:HF-RPL18-GFP construct.

Funding

This work was supported by a grant by the Alexander von Humboldt Foundation to M.V.

Conflict of interest statement. The authors declare no conflict of interest.

References

Bellini C, Pacurar DI, Perrone I (2014) Adventitious roots and lateral roots: similarities and differences. Annu Rev Plant Biol **65:** 639–666

Bogdanovic J, Mojovic M, Milosavic N, Mitrovic A, Vucinic Z, Spasojevic I (2008) Role of fructose in the adaptation of plants to cold-induced oxidative stress. Eur Biophys J **37:** 1241–1246

Bouzid M, He F, Schmitz G, Häusler R E, Weber A P M, Mettler-Altmann T, De Meaux J (2019) Arabidopsis species deploy distinct strategies to cope with drought stress. Ann Bot **124**: 27–40

Brady SM, Orlando DA, Lee JY, Wang JY, Koch J, Dinneny JR, Mace D, Ohler U, Benfey PN (2007) A high-resolution root spatiotemporal map reveals dominant expression patterns. Science **318**: 801–806

Cartwright DA, Brady SM, Orlando DA, Sturmfels B, Benfey PN (2009) Reconstructing spatiotemporal gene expression data from partial observations. Bioinformatics **25**: 2581–2587

Chardon F, Bedu M, Calenge F, Klemens PA, Spinner L, Clement G, Chietera G, Leran S, Ferrand M, Lacombe B, et al. (2013) Leaf fructose content is controlled by the vacuolar transporter SWEET17 in Arabidopsis. Curr Biol **23:** 697–702

Chen HY, Huh JH, Yu YC, Ho LH, Chen LQ, Tholl D, Frommer WB, Guo WJ (2015a) The Arabidopsis vacuolar sugar transporter SWEET2 limits carbon sequestration from roots and restricts Pythium infection. Plant J **83:** 1046–1058

Chen LQ, Cheung LS, Feng L, Tanner W, Frommer WB (2015b) Transport of sugars. Ann Rev Biochem **84:** 865–894

Chen LQ, Qu XQ, Hou BH, Sosso D, Osorio S, Fernie AR, Frommer WB (2012) Sucrose efflux mediated by SWEET proteins as a key step for phloem transport. Science **335:** 207–211

Cho YH, Yoo SD (2011) Signaling role of fructose mediated by FINS1/FBP in *Arabidopsis thaliana*. PLoS Gen **7:** e1001263

Clough SJ, Bent AF (1998) Floral dip: a simplified method for Agrobacterium-mediated transformation of *Arabidopsis thaliana*. Plant J **16**: 735–743

Comas L, Becker S, Cruz VM, Byrne PF, Dierig DA (2013) Root traits contributing to plant productivity under drought. Front Plant Sci **4**: 442 [PMC][10.3389/fpls.2013.00442] [24204374]

Conn SJ, Hocking B, Dayod M, Xu B, Athman A, Henderson S, Aukett L, Conn V, Shearer MK, Fuentes S, et al. (2013) Protocol: optimising hydroponic growth systems for nutritional and physiological analysis of *Arabidopsis thaliana* and other plants. Plant Methods **9**: 4

Crowe JH, Crowe LM, Carpenter JF, Rudolph AS, Wistrom CA, Spargo BJ, Anchordoguy TJ (1988) Interactions of sugars with membranes. Biochim Biophys Acta **947:** 367–384

Czechowski T, Stitt M, Altmann T, Udvardi MK, Scheible WR (2005) Genome-wide identification and testing of superior reference genes for transcript normalization in Arabidopsis. Plant Physiol **139**: 5–17

De Smet I, Signora L, Beeckman T, Inzé D, Foyer CH, Zhang H (2003) An abscisic acid-sensitive checkpoint in lateral root development of Arabidopsis. Plant J **33:** 543–555

Deak KI, Malamy J (2005) Osmotic regulation of root system architecture. Plant J **43:** 17–28

Dekkers BJ, Schuurmans JA, Smeekens SC (2004) Glucose delays seed germination in *Arabidopsis thaliana*. Planta **218:** 579–588

Eom JS, Chen LQ, Sosso D, Julius BT, Lin IW, Qu XQ, Braun DM, Frommer WB (2015) SWEETs, transporters for intracellular and intercellular sugar translocation. Curr Opin Plant Biol **25:** 53–62

Granot D, David-Schwartz R, Kelly G (2013) Hexose kinases and their role in sugar-sensing and plant development. Front Plant Sci **4:** 44

Guo WJ, Nagy R, Chen HY, Pfrunder S, Yu YC, Santelia D, Frommer WB, Martinoia E (2014) SWEET17, a facilitative transporter, mediates fructose transport across the tonoplast of Arabidopsis roots and leaves. Plant Physiol **164:** 777–789

Hanson J, Smeekens S (2009) Sugar perception and signaling–an update. Curr Opin Plant Biol **12:** 562–567

Hedrich R, Sauer N, Neuhaus HE (2015) Sugar transport across the plant vacuolar membrane: nature and regulation of carrier proteins. Curr Opin Plant Biol **25:** 63–70

Hoekstra FA, Golovina EA, Buitink J (2001) Mechanisms of plant desiccation tolerance. Trends Plant Sci **6:** 431–438

Jones B, Ljung K (2012) Subterranean space exploration: the development of root system architecture. Curr Opin Plant Biol **15:** 97–102

Jung B, Ludewig F, Schulz A, Meißner G, Wöstefeld N, Flügge UI, Pommerrenig B, Wirsching P, Sauer N, Koch W, et al. (2015) Identification of the transporter responsible for sucrose accumulation in sugar beet taproots. Nat Plants **1:** 14001

Julius BT, Leach KA, Tran TM, Mertz RA, Braun DM (2017) Sugar transporters in plants: new insights and discoveries. Plant Cell Physiol **58**: 1442–1460

Keller I, Rodrigues CM, Neuhaus HE, Pommerrenig B (2021) Improved resource allocation and stabilization of yield under abiotic stress. J Plant Physiol **257:**153336

Klemens PA, Patzke K, Deitmer J, Spinner L, Le HR, Bellini C, Bedu M, Chardon F, Krapp A, Neuhaus HE (2013) Overexpression of the vacuolar sugar carrier *At*SWEET16 modifies germination, growth, and stress tolerance in Arabidopsis. Plant Physiol **163:** 1338–1352

Klemens PA, Patzke K, Trentmann O, Poschet G, Büttner M, Schulz A, Marten I, Hedrich R, Neuhaus HE (2014) Overexpression of a proton-coupled vacuolar glucose exporter impairs freezing tolerance and seed germination. New Phytol **202:** 188–197

Klotke J, Kopka J, Gatzke N, Heyer AG (2004) Impact of soluble sugar concentrations on the acquisition of freezing tolerance in accessions of *Arabidopsis thaliana* with contrasting cold adaptation – evidence for a role of raffinose in cold acclimation. Plant Cell Environ **27:** 1395–1404

Koch KE (1996) Carbohydrate-modulated gene expression in plants. Ann Rev Plant Physiol Plant Mol Biol **47:** 509–540

Koevoets IT, Venema JH, Elzenga JTM, Testerink C (2016) Roots withstanding their environment: exploiting root system architecture responses to abiotic stress to improve crop tolerance. Front Plant Sci **7**: 1335

Koncz C, Schell J (1986) The promoter of TL-DNA gene 5 controls the tissue-specific expression of chimaeric genes carried by a novel type of Agrobacterium binary vector. Molec Gen Genet **204**: 383–396

Lastdrager J, Hanson J, Smeekens S (2014) Sugar signals and the control of plant growth and development. J Exp Bot **65:** 799–807

Lavenus J, Goh T, Roberts I, Guyomarc'h S, Lucas M, De Smet I, Fukaki H, Beeckman T, Bennett M, Laplaze L (2013) Lateral root development in Arabidopsis: fifty shades of auxin. Trends Plant Sci **18:** 450–458

Le Hir R, Spinner L, Klemens Patrick AW, Chakraborti D, de Marco F, Vilaine F, Wolff N, Lemoine R, Porcheron B, et al. (2015) Disruption of the sugar transporters *At*SWEET11 and *At*SWEET12 affects vascular development and freezing tolerance in Arabidopsis. Mol Plant **8:** 1687–1690

LeClere S, Schmelz EA, Chourey PS (2010) Sugar levels regulate tryptophan-dependent auxin biosynthesis in developing maize kernels. Plant Physiol **153:** 306–318

Lee HW, Cho C, Kim J (2015) *Lateral Organ Boundaries Domain16* and *18* act downstream of the AUXIN1 and LIKE-AUXIN3 auxin influx carriers to control lateral root development in Arabidopsis. Plant Physiol **168:** 1792–1806

Lee HW, Cho C, Pandey SK, Park Y, Kim MJ, Kim J (2019) LBD16 and LBD18 acting downstream of ARF7 and ARF19 are involved in adventitious root formation in Arabidopsis. BMC Plant Biol **19:** 46

Lineberger RD, Steponkus PL (1980) Cryoprotection by glucose, sucrose, and raffinose to chloroplast thylakoids. Plant Physiol **65:** 298–304

Linke C, Conrath U, Jeblick W, Betsche T, Mahn A, Düring K, Neuhaus HE (2002) Inhibition of the plastidic ATP/ADP-transporter protein primes potato tubers for augmented elicitation of defense responses and enhances their resistance against *Erwinia carotovora*. Plant Physiol **129:** 1607–1615

Martinoia E, Maeshima M, Neuhaus HE (2007) Vacuolar transporters and their essential role in plant metabolism. J Exp Bot **58:** 83–102

Martinoia E, Meyer S, De Angeli A, Nagy R (2012) Vacuolar transporters in their physiological context. Ann Rev Plant Biol **63:** 163–213

Michel BE (1983) Evaluation of the water potentials of solutions of polyethylene glycol 8000 both in the absence and presence of other solutes. Plant Physiol **72**: 66–70

Mishra BS, Singh M, Aggrawal P, Laxmi A (2009) Glucose and auxin signaling interaction in controlling *Arabidopsis thaliana* seedlings root growth and development. PLoS One **4:** e4502

Mustroph A, Zanetti ME, Jang CJH, Holtan HE, Repetti PP, Galbraith DW, Girke T, Bailey-Serres J (2009) Profiling translatomes of discrete cell populations resolves altered cellular priorities during hypoxia in Arabidopsis. Proc Nat Acad Sci USA **106**: 18843–18848

Okushima Y, Overvoorde PJ, Arima K, Alonso JM, Chan A, CHang C, Ecker JR, Hughes B, Lui A, Nguyen D, et al. (2005) Functional genomic analysis of the AUXIN RESPONSE FACTOR gene family members in Arabidopsis thaliana: unique and overlapping functions of ARF7 and ARF19. Plant Cell **17:** 444–463

Okushima Y, Fukari H, Onoda M, Theologis A, Tasaka M (2007) ARF7 and ARF19 regulate lateral root formation via direct activation of *LBD/ASL* genes in Arabidopsis. Plant Cell **19**: 118–130

Quick P, Siegl G, Neuhaus E, Feil R, Stitt M (1989) Short-term water stress leads to a stimulation of sucrose synthesis by activating sucrose-phosphate synthase. Planta **177**: 535–546

Patzke K, Prananingrum P, Klemens PAW, Trentmann O, Martins Rodrigues C, Keller I, Fernie AR, Geigenberger P, Bölter B, Lehmann M, et al. (2019) The plastidic sugar transporter pSuT influences flowering and affects cold responses. Plant Physiol **179:** 569–587

Péret B, De Rybel B, Casimiro I, Benková E, Swarup R, Laplaze L, Beeckman T, Bennett MJ (2009) Arabidopsis lateral root development: an emerging story. Trends Plant Sci **14:** 399–408

Pommerrenig B, Ludewig F, Cvetkovic J, Trentmann O, Klemens PAW, Neuhaus HE (2018) In concert: orchestrated changes in carbohydrate hmeostasis are critical for plant abiotic stress tolerance. Plant Cell Physiol **59:** 1290–1299

Pommerrenig B, Müdsam C, Kischka D, Neuhaus HE (2020) Treat and trick: common regulation and manipulation of sugar transporters during sink establishment by the plant and the pathogen. J Exp Bot **71**: 3930–3940

Porco S, Larrieu A, Du Y, Gaudinier A, Goh T, Swarup K, Swarup R, Kuempers B, Bishopp A, Lavenus J, et al. (2016) Lateral root emergence in Arabidopsis is dependent on transcription factor LBD29 regulation of auxin influx carrier LAX3. Development **143:** 3340–3349

Rodrigues CM, Müdsam C, Keller I, Zierer W, Czarnecki O, Corral JM, Reinhardt F, Nieberl P, Fiedler-Wiechers K, Sommer F, et al. (2020) Vernalization alters sink and source identities and reverses phloem translocation from taproots to shoots in sugar beet. Plant Cell **32**: 3206–3223

Rolland F, Baena-Gonzalez E, Sheen J (2006) Sugar sensing and signalling in plants: conserved and novel mechanisms. Ann Rev Plant Biol **57:** 675–709

Rolland F, Moore B, Sheen J (2002) Sugar sensing and signaling in plants. Plant Cell **14:** 185–205

Rosa M, Prado C, Podazza G, Interdonato R, González JA, Hilal M, Prado FE (2009) Soluble sugars—metabolism, sensing and abiotic stress: a complex network in the life of plants. Plant Sign Behav **4:** 388–393

Ruan YL (2012) Signaling role of sucrose metabolism in development. Mole Plant **5:** 763–765

Ruan YL (2014) Sucrose metabolism: gateway to diverse carbon use and sugar signaling. Ann Rev Plant Biol **65:** 33–67

Sauer N (2007) Molecular physiology of higher plant sucrose transporters. FEBS Lett **581:** 2309–2317

Sheen J, Zhou L, Jang JC (1999) Sugars as signalling molecules. Curr Opin Plant Biol **2:** 410–418

Steinbeck J, Fuchs P, Negroni YL, Elsässer M, Lichtenauer S, Stockdreher Y, Feitosa-Araujo E, Kroll JB, Niemeier JO, Humberg C, et al. (2020) In vivo NADH/NAD^+ biosensing reveals the dynamics of cytosolic redox metabolism in plants. Plant Cell **32:** 3324–3345

Takahashi F, Sato-Nara K, Kobayashi K, Suzuki M, Suzuki H (2003) Sugar-induced adventitious roots in Arabidopsis seedlings. J Plant Res **116:** 83–91

Tjaden J, Möhlmann T, Kampfenkel K, Henrichs G, Neuhaus HE (1998) Altered plastidic ATP/ADP-transporter activity influences potato (*Solanum tuberosum*) tuber morphology, yield and composition of tuber starch. Plant J **16:** 531–540

Verslues PE, Agarwal M, Katiyar-Agarwal S, Zhu J, Zhu JK (2005) Methods and concepts in quantifying resistance to drought, salt and freezing, abiotic stresses that affect plant water status. Plant J **45**: 523–539

Vu DP, Martins Rodrigues C, Jung B, Meissner G, Klemens PAW, Holtgräwe D, Fürtauer L, Nägele T, Nieberl P, Pommerrenig B, et al. (2020) Vacuolar sucrose homeostasis is critical for plant development, seed properties, and night-time survival in Arabidopsis. J Exp Bot **71:** 4930–4943

Ursache R, Andersen TG, Marhavý P, Geldner N (2018) A protocol for combining fluorescent proteins with histological stains for diverse cell wall components. Plant J **93**: 399–412

Wahl V, Ponnu J, Schlereth A, Arrivault S, Langenecker T, Franke A, Feil R, Lunn JE, Stitt M, Schmid M (2013) Regulation of flowering by trehalose-6-phosphate signaling in *Arabidopsis thaliana*. Science **339:** 704–707

Wang L, Ruan YL (2013) Regulation of cell division and expansion by sugar and auxin signaling. Front Plant Sci **4:** 163–163

Weichert N, Saalbach I, Weichert H, Kohl S, Erban A, Kopka J, Hause B, Varshney A, Sreenivasulu N, Strickert M, et al. (2010) Increasing sucrose uptake capacity of wheat grains stimulates storage protein synthesis. Plant Physiol **152:** 698–710

Wingenter K, Schulz A, Wormit A, Wic S, Trentmann O, Hörmiller II, Heyer AG, Marten I, Hedrich R, Neuhaus HE (2010) Increased activity of the vacuolar monosaccharide transporter TMT1 alters cellular sugar partitioning, sugar signalling and seed yield in Arabidopsis. Plant Physiol **154:** 665–677

Winter D, Vinegar B, Nahal H, Ammar R, Wilson GV, Provart NJ (2007) An "electronic fluorescent pictograph" browser for exploring and analyzing large-scale biological data sets. PLoS One **2**: e718

Wormit A, Trentmann O, Feifer I, Lohr C, Tjaden J, Meyer S, Schmidt U, Martinoia E, Neuhaus HE (2006) Molecular identification and physiological characterization of a novel monosaccharide transporter from Arabidopsis involved in vacuolar sugar transport. Plant Cell **18:** 3476–3490

Xiong L, Wang RG, Mao G, Koczan JM (2006) Identification of drought tolerance determinants by genetic analysis of root response to drought stress and abscisic acid. Plant Physiol **142:** 1065–1074

Yu H, Chen X, Hong YY, Wang Y, Xu P, Ke SD, Liu HY, Zhu JK, Oliver DJ, Xiang CB (2008) Activated expression of an *Arabidopsis* HD-START protein confers drought tolerance with improved root system and reduced stomatal density. Plant Cell **20:** 1134–1151

Zhan A, Schneider H, Lynch JP (2015) Reduced lateral root branching density improves dought tolerance in maize. Plant Physiol **168:** 1603–1615